UC San Diego
UC San Diego Electronic Theses and Dissertations

Title

Analysis of Vascular Changes after Peripheral Nerve Decompression

Permalink

https://escholarship.org/uc/item/2np92157

Author

Patel, Nevil Gautamkumar

Publication Date

2022

Peer reviewed|Thesis/dissertation

UNIVERSITY OF CALIFORNIA SAN DIEGO

Analysis of Vascular Changes after Peripheral Nerve Decompression

A Thesis submitted in partial satisfaction of the requirements
for the degree Master of Science

in

Biology

by

Nevil Gautamkumar Patel

Committee in charge:

　　Professor Sameer Bhrugu Shah, Chair
　　Professor Cory Matthew Root, Co-Chair
　　Professor Brenda L Bloodgood

2022

The Thesis of Nevil Gautamkumar Patel is approved, and it is acceptable in quality and form for publication on microfilm and electronically.

University of California San Diego

2022

TABLE OF CONTENTS

LIST OF FIGURES

LIST OF TABLES

ACKNOWLEDGEMENTS

I would like to take this opportunity to acknowledge those who have allowed me to produce this research and have contributed to my thesis. Dr. Sameer Shah, my PI has given me endless support and encouragement during my time in his lab and has helped me produce this work despite the conditions of the COVID-19 pandemic. I would also like to acknowledge my committee members Dr. Cory Root and Dr. Brenda Bloodgood for their invaluable input throughout my master's program.

I deeply thank the other Shah Lab members: Yuanshan Wu and Elizabeth Orozco for their assistance and guidance during the surgical procedures that allowed me to finish my thesis.

I would also like to acknowledge the UC San Diego Biology Department for giving me an opportunity to further my research career by completing this thesis. I would also like to recognize the Veterans Affairs Hospital in San Diego and their research staff for allowing me to conduct the necessary surgeries for my master's thesis. I would also love to thank my friends and family for supporting me and encouraging me to do my best during my time in the master's program here at UCSD.

This thesis is currently being prepared for submission for publication of the material. Patel, Nevil; Wu, Yuanshan; Shah, Sameer. "Analysis of Vascular Changes After Peripheral Nerve Decompression." The thesis author is the primary investigator for this material.

ABSTRACT OF THE THESIS

Analysis of Vascular Changes after Peripheral Nerve Decompression

by

Nevil Gautamkumar Patel

Master of Science in Biology

University of California San Diego, 2022

Professor Sameer Bhrugu Shah Chair
Professor Cory Matthew Root, Co-Chair

Cubital tunnel syndrome is an example of a nerve entrapment syndrome where the ulnar nerve is compressed by the surrounding muscles and tissues of the cubital tunnel. Symptoms of peripheral nerve entrapment include pain, numbness, and reduced motor function. Peripheral nerve decompression is one clinical management strategy for nerve entrapment syndromes that involves physically decompressing the nerve from its surrounding muscle and tissues in order the reduce the compression that is experienced by the nerve. The vascular changes that occur to the

endogenous and exogenous vascular systems of peripheral nerves following peripheral nerve decompression are not fully understood. In this study, blood perfusion measurements were recorded via laser doppler flowmetry before and after peripheral nerve decompression in the sciatic nerves of rats. We found that peripheral nerve decompression resulted in a significant decrease in blood perfusion to the distal portion of sciatic nerve that is under tension. However, these vascular deficits were reversed within 6 weeks after the decompression surgery. This study is intended to display the unintended effects on the vascular system following peripheral nerve decompression.

INTRODUCTION

The human nervous system is responsible for a host of sensory and motor functions and is split into two divisions: the central nervous system (CNS), which consists of the brain and the spinal cord, and the peripheral nervous system (PNS), which consists of the remaining peripheral nerves that are distributed throughout the body. The peripheral nervous system relays information such as external stimuli to the brain and motor information to the rest of the body (Menorca et al., 2013). Nerves, the functional units of the peripheral nervous system, facilitate electrical transmission using action potentials that allow communication between different parts of the body (Menorca et al., 2013). Since there is less protection for the nerves in the peripheral nervous system compared to the central nervous system, the PNS and its nerves are at a higher risk for injury (Schmidt & Leach, 2003).

Peripheral nerve injury (PNI) research is crucial as traumatic events or chronic overuse of muscles can disrupt peripheral nerve function which results in sensorimotor dysfunction and pain (Gordon, 2020; Wang et al., 2019). Nerves display natural plasticity on a small scale and can sometimes heal after injury. However, there are several cases where surgical intervention is required to assist in the healing of injured nerves. Research focuses on axonal health, the integrity of nerve projections, along with electrophysiological properties, or the nerve's ability to conduct action potentials, when describing peripheral nerve injury (Burnett & Zager, 2004). Classification of various grades of injury are dependent on axonal integrity, electrophysiology, and vascular damage (Caillaud et al., 2019; SUNDERLAND, 1951). Vascular function as it relates to various types of PNI is an understudied area of research.

1

Vascular System of Peripheral Nerves

The nerves of the peripheral nervous system have a unique vascular structure that supports neuronal health. The vascular system consists of two systems: exogenous and endogenous (Caillaud et al., 2019). The exogenous blood supply is composed of small veins/arteries that originate from the surrounding muscle and tissue that penetrate the epineurium, the outermost layer of the nerve (Caillaud et al., 2019). Inside the perineurium, which can be considered the middle layer of the nerve, there are arterioles, arteries, venules, and capillaries between the individual nerve fibers that feed into those specified nerve tracts to form longitudinally arranged capillaries creating the microvascular environment (Caillaud et al., 2019). The endogenous vascular system consists of the tracts that will then cross into the endoneurium, the innermost layer, of individual nerve fibers to provide them with blood flow (Caillaud et al., 2019). As nerves are highly metabolic structures, injuries to peripheral nerves may change the vascular environment which in turn could have consequences in terms of peripheral nerve injury recovery and overall nerve health (Best & Mackinnon, 1994; Zamir et al., 2012).

Cubital Tunnel Syndrome and Nerve Decompression

There are a few categories of damage that affect peripheral nerves. These categories include nerve compression, nerve transection/lacerations, and stretch related injuries (Burnett & Zager, 2004; Caillaud et al., 2019; Chhabra et al., 2014; SUNDERLAND, 1951). Certain degrees of peripheral nerve injury can result in the sensorimotor deficits and systemic pain. Cubital tunnel syndrome (CBTS) is an example of a nerve compression or nerve entrapment syndrome. CBTS is the compression of the ulnar nerve and is the second most common peripheral neuropathy of the upper extremities (Burahee et al., 2021; Freund et al., 2021).

Current theories involving the progression of cubital tunnel syndrome suggest that the ulnar nerve is compressed by the surrounding muscles and tissue of the cubital tunnel near the elbow (Aleem et al., 2014; Freund et al., 2021). The ulnar nerve has sensory and motor functions and originates from C8 and T1 from the spinal cord and travels down the arm posteriorly through an area called the cubital tunnel to finally extend to the ulna (Guru et al., 2015). Compression of the ulnar nerve interferes with its ability to glide along the cubital tunnel which leads to specific regional strain of the nerve (I. Foran et al., 2016).

In terms of injury management, there are two procedures that can be performed for cubital tunnel syndrome: anterior subcutaneous transposition and peripheral nerve decompression (Burahee et al., 2021; Freund et al., 2021). Anterior subcutaneous transposition involves transposing the nerve or repositioning the nerve that releases pressure around the nerve but changes its anatomical course (Burahee et al., 2021; Freund et al., 2021). Peripheral nerve decompression is similar to anterior subcutaneous transposition in terms of relieving pressure, but peripheral nerve decompression only relieves the anatomical barriers in the cubital tunnel and the surrounding tissues, so the anatomical course of the ulnar nerve is unchanged (I. Foran et al., 2016). These two techniques have been critically evaluated and have been shown to produce similar clinical outcomes for patients affected with cubital tunnel syndrome. However, there are still several patients who report that these procedures do not alleviate symptoms. The incidence rate for patients whose symptoms do not resolve is up to 50% (Aleem et al., 2014). Although peripheral nerve decompression is a safe procedure and has an acceptable success rate in alleviating CBTS, it should be critically evaluated for why symptoms return in certain individuals following the procedure.

The biomechanics of the ulnar nerve have been evaluated post-decompression in patients with CBTS and it has been shown that there are increased amounts of nerve strain in the distal portion of the ulnar nerve in certain configurations of the elbow and wrist (I. Foran et al., 2016). Furthermore, in rat studies where peripheral nerve decompression was performed on the sciatic nerve, higher levels of strain were detected due to the tension the nerve experiences because of knee/ankle configurations (I. M. Foran et al., 2018). Clearly, decompression and tension are factors that alter the amount of strain the nerve experiences and could have potential effects on the function of nerves themselves.

Peripheral nerve decompression, in theory, should not alter nerve structure and health as there is no axonal disruption of the nerve. The decompression usually involves separating the nerve from its nerve bed (typically a fatty connective tissue layer adjacent to underlying and overlying muscle) to relieve compression. Given the anatomy of the neurovascular system, there is clear potential for damage to the vascular systems that supply the ulnar nerve or any nerve when peripheral nerve decompression is performed. When there is existing compression on the nerve, blood flow is reduced and may disturb oxygen distribution throughout the nerve (Prevel et al., 1993). The vascular damage that occurs following peripheral nerve decompression should be in question. During anterior transposition, if the ulnar nerve is excessively released from its nerve bed, there can be a potential to negatively affect the blood supply that leads into the ulnar nerve (Li et al., 2015). This risk should be taken into consideration as vascular system disruption and remodeling may have an impact on nerve regeneration/nerve function after nerve decompression.

The first section of this thesis will contain a general review of peripheral nerve injury with an emphasis on the vasculature and its remodeling. The second half of this thesis will

4

contain data from my project that investigates peripheral nerve decompression and its effect on

blood perfusion.

LITERATURE REIVEW: VASCULAR REMODELING DURING NERVE INJURY AND
REPAIR

Introduction

The nervous system is subdivided into the central nervous system and the peripheral
nervous system. The peripheral nervous system houses the many sensory, sympathetic, and
motor neurons that are responsible for sensorimotor function. Given their superficial location,
anatomical course, and dynamic mechanical and chemical environment, peripheral nerves are
susceptible to damage. Nerve damage is a common occurrence, whether via overuse, disease, or
trauma and can result in sensorimotor impairment and systemic pain (Arányi et al., 2018; Burnett
& Zager, 2004; Čebašek & Ribarič, 2016; Jou et al., 2000; Wang et al., 2019). Unfortunately,
outcomes are often poor for more severely injured nerves, and so regeneration remains a major
challenge despite the fact that axons may display some natural outgrowth (1-2.mm/day)(Schmidt
& Leach, 2003). For severed axons, literature supports a model in which nerves regenerate
through the sequential processes of Wallerian degeneration in the distal stump, regrowth of
proximal axons into and past the distal stump, and ultimately, end-organ reinnervation and
recovery (Best & Mackinnon, 1994; Burnett & Zager, 2004; Caillaud et al., 2019; Menorca et al.,
2013). Though there is increasing insight into the factors that regulate axonal regeneration, an
aspect that is often overlooked is how the vasculature, or the blood supply, of nerves participates
in nerve regeneration. Indeed, Caillaud et al. states that "little is known about the specific role of
revascularization in nerve regeneration" (Caillaud et al., 2019) . Given that nerves are
metabolically active and highly vascular, such a contribution from the vascular system may be
especially important (Zamir et al., 2012). The scope of this literature review is to summarize
vascular roles in normal nerve function, vascular remodeling after peripheral nerve injury, and

potential treatment strategies that may enhance neurovascular recovery. While vascularity no doubt influences the progression of several neuropathies, including entrapment neuropathies, diabetic neuropathy, and chemotherapy induced neuropathy this review primarily focuses on traumatic nerve injury. Diabetic neuropathy will not be discussed in this literature review; if more information is needed, Said et al. contains a comprehensive literature review on the various types of neuropathies that plague the peripheral and central nervous system (Said, 2007).

Vascular System Structure

To understand vascular roles in peripheral nerve damage and repair, it is first important to understand the complex anatomy of the microvasculature of peripheral nerves. The vascular system supporting peripheral nerves, such as the sciatic nerve, is composed of two systems: exogenous and endogenous. The endogenous blood supply consists of the arterioles, arteries, venules and capillaries between the individual nerve fibers that feed into specific nerve tracts, enabling a network of longitudinally arranged capillaries creating the microvascular environment (Best & Mackinnon, 1994; Gao et al., 2013). The exogenous blood supply consists of small veins/arteries that originate from surrounding tissue space/muscular blood vessels and is located within the loose connective tissues around the epineurium (Best & Mackinnon, 1994; Gao et al., 2013). Those vessels from the exogenous vascular system are suggested to penetrate the epineurium and travel into and along the perineurium, where they further penetrate the endoneurium and interconnect to the endogenous vascular system. The perineurium serves as a selective barrier to exclude certain proteins and large macromolecules to maintain homeostasis of the endogenous vascular system (Caillaud et al., 2019). Depending on the severity and type of peripheral nerve injury, the epineurium, perineurium, and endoneurium all have the potential to sustain damage.

Relevance of Vascular Structure to Grading of Nerve Injury

Clinically, physicians have primarily relied on two scales for categorizing nerve damage: Seddon and Sunderland Classifications (Chhabra et al., 2014; SUNDERLAND, 1951). The Seddon classification system primarily focuses on the continuity of the axon and has three categories while the Sunderland classification system is broken down into five grades as it considers the health of the epineurium, perineurium, and endoneurium (SUNDERLAND, 1951).

The Seddon classification system was developed by Sir Herbert Seddon in 1943 (SEDDON, 1943). The Seddon classification system involves sorting nerve injuries into three categories: neurapraxia, axonotmesis, and neurotmesis (Menorca et al., 2013; SUNDERLAND, 1951). Neurapraxia is characterized by the presence of demyelination at the injury site (Menorca et al., 2013). Due to the damage to the myelin sheath, nerve conduction velocity is reduced or blocked (Menorca et al., 2013). Recovery from neurapraxia can range from 2-3 months as axonal integrity is unaffected (Caillaud et al., 2019; Maugeri et al., 2021). Axonotmesis is characterized by partial axonal disruption and the presence of nerve growth factors that are released from the distal end (Caillaud et al., 2019; Menorca et al., 2013). These nerve growth factors communicate to the proximal end of the nerve injury to produce axonal sprouts for recovery. For low grade axonotmesis, if function does not recover, surgical intervention may be required (Menorca et al., 2013). Finally, neurotmesis presents itself as a complete disruption of the nerve most referred to as a nerve transection (Gordon, 2020). Surgical intervention through end-to end repair or using a graft is necessary for nerve injuries classified under neurotmesis (Gordon, 2020; Schmidt & Leach, 2003). This classification system is useful in diagnosing nerve damage; however, it does not take into consideration the potential vascular damage that occurs in peripheral nerve injury.

The Sunderland classification system was developed as an expansion to the Seddon classification system. Five grades were used to further distinguish the degree of damage that

occurs during nerve injury. The ability for the nerve to return to normal function after injury, is

dependent on the grade of the injury the nerve has sustained, with increasing severity correlating

with poor outcomes. This scale will be more pertinent for this review as it will discuss some of

the vascular structures that are prominent in peripheral nerves. While vascular impacts of varying

degrees of injury are implied in injury classification systems, such impacts have not been directly

measured or defined.

The first grade of Sunderland's scale is characterized by alterations of the myelin sheath

or segmental demyelination while exhibiting minor axonal and connective tissue damage. Nerve

compression or nerve trunk compression is an example of a grade 1 injury, and the nerve will not

exhibit complete loss of both motor and sensory functions as nerve continuity is structurally

intact (Burnett & Zager, 2004; Maugeri et al., 2021). The concern with this grade of injury is

usually some degree of motor deficiency and neuropathic pain. In most cases of grade 1 nerve

damage, vascular impairment is expected to be minimal as the epineurium, perineum, and the

endoneurium are all intact (Caillaud et al., 2019; SUNDERLAND, 1951). On the other hand,

there is the possibility that the extrinsic vascular system could be impacted; thus, damage to

neural elements may be decoupled from vascular impacts on nerve function. Crush injuries may

be categorized into grades 2-4 depending on the severity (Caillaud et al., 2019). This severity in

turn likely influences the extent of vascular damage. Grade 2 is characterized by the partial loss

of axon continuity and further demyelination. As there is no damage to connective tissue

structures associated with nerve fibers, no damage to major vessels is expected in Grade 2. On

the other hand, Grade 3 displays damage to the endoneurial tubes accompanied with axonal

degradation and Wallerian Degeneration, and thus may result in damage to capillary networks.

Grade 4 is categorized by damage to the perineurium (SUNDERLAND, 1951), thus raising the

possibility of damaging arterioles, venules, and small arteries and veins. Finally, Grade 5 is used for nerves that exhibit complete loss of nerve continuity such as lacerations to the nerve. As it is a nerve laceration, there is likely major damage to all internal and external vascular structures, including those within and flanking the epineurium (Caillaud et al., 2019; Chhabra et al., 2014). The likelihood of any form of recovery happening is dependent on the distance between the proximal and distal stumps. If that distance is smaller, there is a higher chance of nerve regeneration. Surgical intervention is required for most grade 5 nerve injuries. From the classification of injury, it is predicted that the vascular system will sustain heavy damage as there is loss of continuity of all longitudinal vascular structures.

Importance of Vascularity to Wallerian Degeneration and Nerve Regeneration

Wallerian Degeneration is the systematic remodeling of the distal stump following nerve fiber transection (Caillaud et al., 2019). The first stages prioritize the removal of axonal and myelin debris so the nerve can remove damaged tissue so healing may begin. Schwann cells release factors such as MCP-1 (monocyte chemoattract protein-1), NGF (neuronal growth factor), CTNF, BDNF, GDNF and others (Burnett & Zager, 2004; Caillaud et al., 2019). MCP-1 plays a crucial role in recruiting macrophages to the injury site after being released from the Schwann cells. These macrophages are responsible for axonal phagocytosis and the clearance of myelin debris. An early increase in permeability can be detected as the nerve is attempting to clear the debris from the endoneurium, promoting greater blood nerve exchange as the nerve heals (Burnett & Zager, 2004). Among the consequences of such exchange, circulating monocytes will differentiate into various macrophages for two weeks after injury after injury (Rotshenker, 2011). These activated macrophages will then contribute to Wallerian degeneration by further removing debris from the axon and myelin sheath. This amplification of clearance is

crucial to create a favorable microenvironment for structural regeneration of the nerve. Nissl

bodies will form from the breakdown of rough endoplasmic reticulum, promoting synthesis of

new proteins (Alvites et al., 2018), including cytoskeletal-associated proteins such as myosin and

actin that will provide structural support for the regenerating nerve (Renno et al., 2017).

Remodeling of the vascular system will accompany this structural regeneration of nerve axons,

providing metabolic support. In addition, macrophages entering the regenerative milieu are also

responsible for the release of vascular endothelial growth factor, otherwise known as VEGF (Wu

et al., 2021). VEGF is a crucial factor as it starts the process of angiogenesis and the clotting

cascade to promote vascular remodeling during nerve recovery (Ding et al., 2009; Wu et al.,

2021). In addition to supporting early phases of nerve stabilization and recovery, vascular

function is also required to support subsequent axonal regeneration. A growth cone will be

formed at the distal end of the proximal bud and will release filopodia to detect the

microenvironment a couple of hours after injury (Geraldo & Gordon-Weeks, 2009). These

filopodia will make their way to the distal stump upregulating structural proteins such as actin

and myosin to begin rebuilding the axon (Costigan et al., 1998). As the growth tube reaches the

endoneurial tube, the functional completion of recovery is achieved once remyelination, axon

enlargements, and functional reinnervation occur. Although neighboring Schwann cells carry out

remyelination, the full remyelination of an axon is unlikely due to those Schwann cells having

insufficient stimulation of neural growth factors via the Schwann cells. One point to note is that

the thickness of the myelin during remyelination along with axonal integrity may not be the same

pre-injury which can lead to diminished electrical signaling in the axon (Modrak et al., 2020).

     Finally, metabolic and trophic support is also required for the final stages of regeneration

required for functional recovery, end-organ reinnervation. Once the axon has extended a

sufficient length, end-organ recovery is facilitated via the stabilization of the neuromuscular

junction. For active remodeling to occur, a blood supply is needed for the clearance of debris,

delivery of growth factors, oxygen delivery to mitochondria, and stabilization of the

neuromuscular junction (Podhajsky & Myers, 1993). Thus, from beginning to end, the success of

nerve regeneration is contingent on a suitable microenvironment being formed through the

clearing of debris, the release of neurotrophic factors, and vascular remodeling (Podhajsky &

Myers, 1993).

Vascular Response to Injury/Vascular Remodeling

The vascular networks within nerve tracts are susceptible to remodeling upon changes in

nerve length or injury. Schwann cells are concentrated in the endoneurium and are responsible

for releasing a host of growth factors to aid in nerve regeneration and vascular remodeling

(Podhajsky & Myers, 1993). Like the function of axonal growth cones in axonal regeneration,

there are specialized tip cells that respond to VEGF that allow for sprouting of capillaries and

regulate vascular branching (Adams & Eichmann, 2010). Both axonal growth cones and these

vascular tip cells produce signaling cues for vascular remodeling. There is a protective barrier

called the blood nerve barrier that separates the vascular component from the nerve tissue itself

and has low permeability due to tight junctions that are the end of both the perineurium and the

capillary. Abnormalities in the blood nerve barrier or the endoneurial composition of a particular

nerve can be associated with trauma, compression, and toxins (Rechthand & Rapoport, 1987)

There is a rather extensive understanding of the organization of peripheral vasculature.

However, despite the fact that there is most likely an association between vascularization and

nerve regeneration (Muangsanit et al., 2018), there are far fewer studies exploring the effects of

how the regeneration of the endogenous and exogenous vascular systems affect nerve regrowth after damage.

Currently, it is known that there are two phases to describe the vascular reaction to peripheral nerve injury. The first phase consists of an increase in vascular radius and perimeter but a decrease in vessel number and density one week after injury while the second phase, seen at 6 weeks post-injury shows an increase in vessel density and number within the regenerating nerve front (Podhajsky & Myers, 1993). Large and Tyler state that 6-8 weeks post injury is when the nerve has been reinnervated and the capillary distribution has been reorganized and can accommodate different metabolic needs for fibers (Large & Tyler, 1985).

Factors affecting Regeneration

Gao et al. mentions the current methods to improve vascular healing after an injury usually include surgery, the addition of vasoactive factors and physical therapy (Gao et al., 2013). In the current literature, there have been certain molecular factors that have been associated with vascularization, that may underlie such phenomena.

Netrin-1 is a pro-angiogenic factor that is produced by arterial smooth muscle. Netrin-1 is a laminin-related diffusible protein that was described as a guide protein for neurogenesis as it attracts/repels the axonal growth cones (Castets & Mehlen, 2010). It has also been shown that arterial vessel innervation requires Netrin-1 interaction with its receptors that are apparent on sympathetic growth cones (Castets & Mehlen, 2010). The mechanism on which Netrin-1 acts is through inducing the stimulation of proliferation amongst target cells and promoting the differentiation and migration of capillaries (Castets & Mehlen, 2010) As it aids in growth of vascular structures such as capillaries, Netrin-1 is a promising factor that could be delivered with a host of other factors to improve vascular remodeling after injury.

VEGF is another factor that can bring about an angiogenic response, which is the growth of blood vessels after injury. Momhammadi et al. have shown that VEGF overexpression is key to pathological and functional repair of sciatic nerve crush injury (Mohammadi et al., 2013) Even though some studies have observed this link, other studies disagree on the impact. Hobson et al. explored the effects of dosage-dependent VEGF on Lewis rats that had undergone injury to the sciatic nerve via needle puncture at the proximal nerve stump. rhVEGF was shown to increase vascularization which was associated with an increase in nerve regeneration and that VEGF's vascular response was dose dependent (HOBSON et al., 2000). They acknowledge that studies have not been conclusive whether nerve regeneration might be enhanced by vascularization via VEGF but accept that VEGF has been known to have protective effects against neurodegeneration (HOBSON et al., 2000). Mice were mutated through a targeted deletion of the promoter of the VEGF gene, so VEGF levels were lower than the control. These mice with the VEGF mutation were shown to develop adult-onset motor neuron degeneration which is similar to ALS (amyotrophic lateral sclerosis). A 50% decrease in VEGF was shown to be detrimental to angiogenesis and was shown to interfere with neural perfusion (Niu & Chen, 2010). VEGF has a host of effects including aiding in axonal regrowth, stimulation of growth of Schwann cells. amplified neurogenesis, prevention of axonal and myelin degradation, etc. VEGF is a promising candidate to study for vascular remodeling as the current literature supports that VEGF has many-angiogenic effects. VEGF's mechanism of action and effect on capillary density and capillary permeability is a potential area of study that may further the discussion on vascular remodeling in peripheral nerve injuries.

NGF (neuronal growth factor) is also another potential source of revascularization and nerve regeneration. In one study, collagen tubes that released NGF were used combat peripheral

nerve injury was found to show promising outcomes in terms of nerve regeneration (Long et al., 2021). In another study, DNA hydrogels that were infused with VEGF and NGF were used to assist in peripheral nerve injury recovery in rats (Liu et al., 2021). Similarly, VEGF+NGF delivery via a nanofibrous scaffold showed increased vascularization as well as nerve regeneration post-operation of rat sciatic nerves (Xia & Lv, 2018). NGF is another crucial factor that effects the regeneration of nerves and while improving vascular health.

Basic fibroblast growth factor (bFGF) is another factor that has been shown to increase vascular remodeling. A study found the bFGF delivered via emulsion scaffolds promoted high levels of vascular remodeling and increased levels of blood perfusion in mice (Moncion et al., 2017). Mesenchymal stem cells that were expressing bFGF was found to increase both micro vessel density and VEGF expression when delivered via transplantation in rat models that displayed hind limb ischemia (Zhang et al., 2014). Basic fibroblast growth factor is another factor that has been shown increase vascularity and should be considered as a potential factor to partner with other factors discussed above to increase vascular remodeling for future peripheral nerve experiments.

Methods of Evaluating Nerve Vasculature

Given the increased attention to vascular impacts on nerve regeneration, it is worthwhile to understand strengths and limitations of current strategies for evaluating structural and functional vascular outcomes.

Immunohistochemical staining is a well-established "pathology-like" approach to quantify blood vessels in animal models of nerve degeneration and regeneration. These staining techniques offer qualitative assessments of overall vascular distribution as well as quantitative

15

outcomes related to dimension. However, classically, as approaches are typically limited to cross sections or longitudinal sections, a proper three-dimensional perspective is lacking.

Microcomputed Tomography can provide visualization of micro vessels while simultaneously imaging the volume of these vessels in three dimensions (T. M. Saffari, Mathot, Bishop, et al., 2020). This method typically works through imaging fluorescent or analogous contrast-enhancement compounds that have been perfused throughout the animal's body (T. M. Saffari, Mathot, Bishop, et al., 2020). Alternatively, thicker tissue sections labeled with antibodies may be visualized through other volumetric imaging strategies (e.g., confocal or multi-photon imaging). Although, conventional photography of perfused structures is more cost-effective, faster, and less equipment-dependent than micro-CT, conventional photography cannot visualize the three-dimension vascular structure of peripheral nerve as effectively as micro-CT (T. M. Saffari, Mathot, Bishop, et al., 2020).

Wide-field microscopy has been used with optical coherence tomography to provide higher resolution of three-dimensional images of the vascular network including intraneural nerves and longitudinal imaging of revascularization and myelination (Nam et al., 2018). Certain methods that utilize wide-field microscopy may have an edge over labeling-based techniques as they do not degrade the vessel permeability while providing the three-dimensional images of vascular networks in recovering nerves (Nam et al., 2018). Although this in-vivo method has been tested in animal models, analyzing vascular damage/recovery in humans would be a great addition for evaluating nerve vascular health.

Magnetic resonance neurography (MRN) is a tool used in diagnosing peripheral nerve injury in clinical settings by imaging thin sections of nerve and the surrounding tissue with high resolution (Chhabra et al., 2014). This method provides great contrast between the various

aspects of muscle and nerve health, while also corresponding with electrophysiological data as well (Chhabra et al., 2014). While this is another powerful tool in imaging and classifying nerve injury in correspondence to Sunderland and Seddon scales, its high-resolution capabilities should be taken advantage to image vascular discontinuities as well.

Laser Doppler Flowmetry is one noninvasive method that can perform rapid measurements on the vascular system. This method is particularly useful in determining transient nerve blood flow in humans (Rundquist et al., 1985). Although LDF is used clinically, there are some limitations to consider. The Doppler signal can display variable readings depending on the depth of the measurement site in question. For example, if a nerve is being measured, overlying fascia may affect the readings as there is inherent scattering of light as the signal passes through layers of tissue (Fagrell & Nilsson, 1995). Furthermore, the heterogeneity of tissues can affect Doppler output. Doppler readings can vary and produce artifacts because of muscle movements and the movement of probe to adjacent sites to the same muscle as well (Fagrell & Nilsson, 1995). However, new methods such as using different laser wavelengths and new techniques such as infrared laser doppler flowmetry have shown promise in combating these issues (Rajan et al., 2009). Laser Doppler Flowmetry is a powerful tool in measuring blood perfusion, but due to the multi-factorial influences on perfusion, since flow itself is not being directly measured, its limitations must be considered when studying the blood perfusion of nerves in both experimental and clinical settings.

Ultrasound is another powerful diagnostic tool used in both clinical and research settings to describe peripheral nerve trauma in humans (Arányi et al., 2018). Literature supports the use of ultrasound in clinical settings along with neurophysiological assessments to precisely diagnose peripheral nerve injury with therapeutic accuracy (Arányi et al., 2018; Padua et al.,

2012). Although contrast enhanced ultrasonography has been used to observe the change in vascularization in patients with penetrating nerve injuries, it is imperative to discover the method's reliability in measuring vascular function with other types of nerve injury. For example, presentation of reduced intraneural blood flow through this method may be a sign of entrapment neuropathies such as cubital and carpal tunnel syndromes (Carroll & Simon, 2020).

These are some, not all, imaging techniques used in field to visualize both nerve damage and vascular damage. Visualization methods that are developed for clinical use will be advantageous along with other methods for assessing nerve health.

New Directions in Research/Treatment

In pre-clinical and clinical models, grafts have been deployed extensively to facilitate nerve regeneration. Autografts of nerves taken from an individual with a peripheral nerve injury and used to assist in surgical nerve repair in that individual. Allografts are like autographs but are taken from another individual/animal's tissue to repair. Xenografts are developed from tissue from another species and modified to assist in nerve repair. Consistent with the importance of vascular roles in promoting structural and functional nerve recovery, there is increasing emphasis on augmenting graft capabilities through vascularization. For example, wrapping the superficial inferior epigastric artery fascia flap around an allograft showed promising results in rats to increase vascular volume when compared to conventional grafts. (T. Saffari et al., 2020; T. M. Saffari, Mathot, Bishop, et al., 2020; T. M. Saffari, Mathot, Friedrich, et al., 2020). A review by Muangsanit et al. has covered the extensive use of vascularized nerve grafts in nerve repair research (Muangsanit et al., 2018).

While not typically released during nerve regeneration, MVSC (multipotent vascular stem cells) may be a less direct treatment option for inducing vascularization. These stem cells

have the potential to differentiate into neural or vascular cell types in regenerating nerves (Huang et al., 2019). MVSC's were shown to form connections within the perineurium assisting in regeneration (Huang et al., 2019). As the perineurium is disrupted during more severe nerve injuries, its repair through an increase in angiogenic processes could potentially aid neurovascular remodeling after nerve injury.

Vascular function may also enhance myelination. Wu et al. (2021) found that delivery of the combination of the angiogenic factor VEGF as well as Schwann cells to injured nerves had better outcomes than model where only VEGF or Schwann cells were delivered. Delivery of combinations of VEGF and Schwann cells were observed to activate the VEGFR2/ERK signaling pathway which contributes to nerve regeneration by differentiating adipose-derived mesenchymal stem cells into endothelial cells that promote lengthening of the regenerating axon (Sun et al., 2018, Wu et al., 2021).)Wu et al., 2021). VEGF delivery through a slow-release sponge in addition to nerve grafts may also aid in accelerating vascular remodeling, thereby increasing the vascular contributions to regeneration after nerve injury (Wu et al., 2021). Schwann cells and VEGF are intertwined in their ability to promote angiogenesis so therapies targeting these two components in parallel may improve vascular remodeling.

Another study has attempted to increase the transcription of VEGF and NGF through pDNA plasmid gene delivery (Fang et al., 2020). This form of gene therapy was linked to better rat sciatic nerve recovery as the VEGF+NGF group had higher amounts of remodeled micro vessels compared to groups who were only given VEGF or only NGF (Fang et al., 2020). Gene therapy that is localized to this degree may provide benefits for those whose peripheral nerve injuries exhibit severe vascular damage.

Although Sunderland and Seddon scales are generally acceptable for defining nerve damage in clinical settings, there are limitations to this scale as there are many instances where certain nerve injuries do not follow the typical patterns. For example, distinguishing grade three injuries that mostly require medical treatment from grade four or five where surgical treatment is a must is quite difficult. A potential reason for this difficulty is that electrophysiological signals can be inconsistent amongst severed nerves. Some nerves display electrical signals that are typically normal for a week after nerve injury. On the other hand, if there is no electrical signal present from the nerve, that alone is not sufficient to determine if a nerve has been severed. These scales should be revisited and revised to form modern scales that effectively quantify nerve injuries from the data produced by current research.

Conclusion

This review served as a brief overview of peripheral nerve injury and recovery. The field of peripheral nerve injury research is truly fascinating. Developments over the last 50 years of research have refined assessment and treatment options of peripheral nerve injury. There is an overwhelming amount of research dedicated to various components, factors and processes that surround the regeneration response to nerve injury. Wallerian Degeneration, axonal degeneration, and end-distal organ recovery are proven to be some of the key processes in nerve regeneration. Vascular remodeling still seems to be an understudied area in this field of research. An argument should be made that since debris clearance and delivery of cells, trophic factors, oxygen, and metabolites via blood vessels are important for nerve health, vascular remodeling after peripheral nerve injury should play a bigger role when deciding the regeneration potential of peripheral nerves.

EXPERIMENTAL PROJECT INTRODUCTION

For my experimental project, I will be examining the changes in blood perfusion (blood-flow) in the sciatic nerve of rats following two potentially interlinked perturbations, nerve tensile stretch via joint movement and nerve decompression. The rat sciatic nerve was chosen for this experiment as it a commonly used model in peripheral nerve injury research (Vela et al., 2020). There are three areas of interest: the surrounding muscle (hamstring) of the sciatic nerve, the proximal sciatic nerve, and the distal sciatic nerve. The rationale for taking measurements from both proximal and distal ends is that there has been a presence of regional differences in terms of mechanical strain due to stretching. The surrounding muscle represents a control. Foran et al. (2016) describes an increase in regional strain in the distal and central portions of the ulnar nerve after peripheral nerve decompression when compared to anterior transposition. To account for the effect stretch can have on the sciatic nerve, there will be measurements recorded in both unstretched and stretched positions of the sciatic nerve. To evaluate effects of decompression, blood perfusion recordings will be collected on day zero, one week, and six weeks post-decompression. The day zero and one-week readings will provide us with immediate, acute vascular changes that may occur after peripheral nerve decompression. The six-week time point will be used to evaluate potential long-term changes in vascular nerve function. Comparisons between day zero blood perfusion and one-week and six-week blood perfusion will be used to display the overall vascular trajectory after peripheral-nerve decompression.

For Immunohistochemistry staining, laminin and beta-tubulin will be used to evaluate axonal health. GLUT1, VEGF, and smooth muscle actin will be used to quantify vasculature and its potential remodeling after peripheral nerve decompression.

We hypothesize that there will be observable differences in blood perfusion following peripheral nerve decompression, as well as vascular remodeling to restore blood perfusion levels post-decompression.
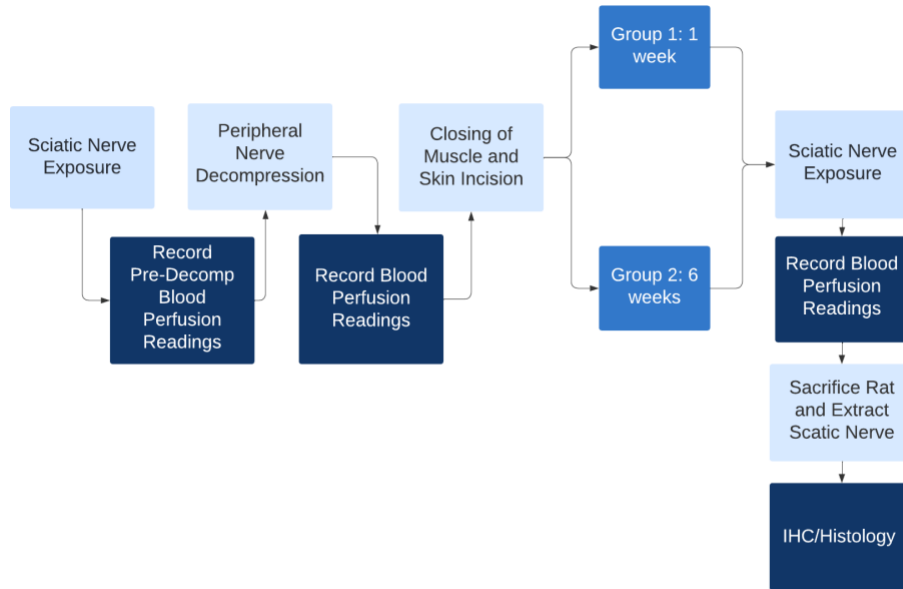
Figure 1: Flowchart displays the experimental method from initial sciatic nerve exposure to sciatic nerve harvest and staining.

Sciatic Nerve Exposure/Decompression

All procedures were approved by the Veterans Affairs Hospital in San Diego, California. Fourteen adult Rattus Norvegicus rats and their sciatic nerves were used in this experiment. Ten rats were used for the collection of Doppler flowmetry data for a primary 6-week time point, and four more rats were used for data collection at a 1-week pilot time point. All surgical tools were sterilized through bead sterilization. Surgical procedures were performed with the rats under isoflurane anesthesia. For initial induction, the rats were placed in an induction box where 2-3% isoflurane was administered. Once the animals were sufficiently anesthetized, they were moved to a nose cone where the same amount of isoflurane was administered during the procedure. Nair was used to remove the hair around the incision site around the leg area located on the posterior side of the rat. Repetitive application of ethanol and chlorhexidine were used to sterilize the

incision site. The following was administered subcutaneously before surgical operation: 1ml of NaCl .9% solution (to prevent dehydration during the operation), Baytril (antibiotics to prevent infection post-operation, 5mk/kg), and Buprenorphine SR (slow-release opioid analgesic for pain relief, 1-1.2mg/kg). During all the procedures, rats were placed on a heating pad to maintain body temperature.

Before any incision was made, the toes on the side of the incision site were pinched to ensure there was no reflex. A sterile scalpel was used to create a small skin incision, approximately 5mm, below the femoral axis. The sciatic nerve was accessed by separating the semitendinosus and the quadriceps femoris muscle (to ensure minimal muscle damage). Sterile forceps were used to lift the sciatic nerve from its nerve bed to simulate peripheral nerve decompression. Special care was taken to perform consistent peripheral nerve decompressions without inflicting unnecessary damage to the sciatic nerve. A Doppler probe from the Perimed 5001 Doppler Flowmetry machine was used to record blood perfusion. After the relevant Doppler Flowmetry readings were taken with the Perimed 5001, the muscle was closed via 8-0 Vicryl suture and the skin incision was closed via surgical staples. Neosporin was applied to the incision site to prevent infection of the surgical site. The rats were taken off isoflurane administration and were placed in post-operative observation. All rats were observed daily for one-week post-operation and weekly until six weeks post-operation. The surgery and Doppler Flowmetry readings were repeated for both groups when their respective time was over. After the final Doppler readings were taken, the rats were sacrificed, and the sciatic nerve and its nerve bed was harvested. All nerve tissue was placed immediately in vials containing 4% paraformaldehyde for tissue fixation for 24-48 hours and then placed in 70% Ethanol for preservation and consequent immunohistochemistry staining.
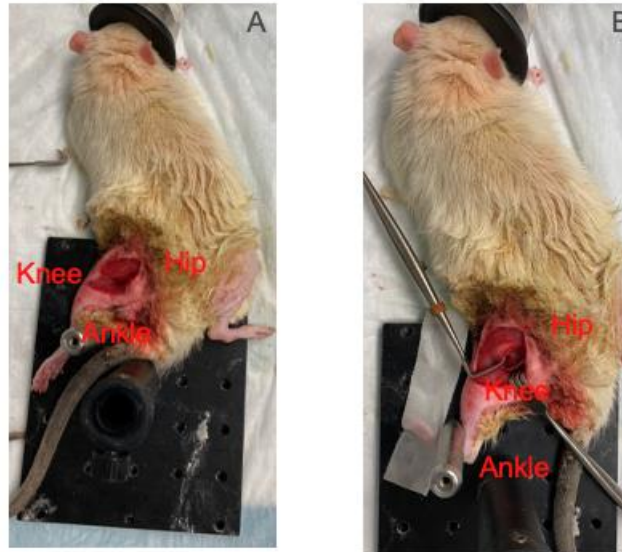
Figure 2: A. Non-Stretched configuration of the sciatic nerve as shown with the knee neutral and the ankle in plantarflexion. B. Stretched configuration of the sciatic nerve as shown with the knee straightened and the ankle in dorsiflexion.

Stretched vs Non-Stretched

In the current literature, stretched peripheral nerves can have different outcomes than non-stretched peripheral nerves (I. Foran et al., 2016; I. M. Foran et al., 2018). Due to the discovery of increased strain in specific portions of the nerve when it is under mechanical tension, we have included stretched and unstretched models in our experimental design. The ankle and knee position of the rat was configured in two conditions: one where the sciatic nerve is stretched and one where the nerve has no tension (non-stretched). In the non-stretched condition, the knee remained bent, and the foot was in plantarflexion. In the stretched condition, the knee was positioned to remain straight, and the foot was in dorsiflexion.
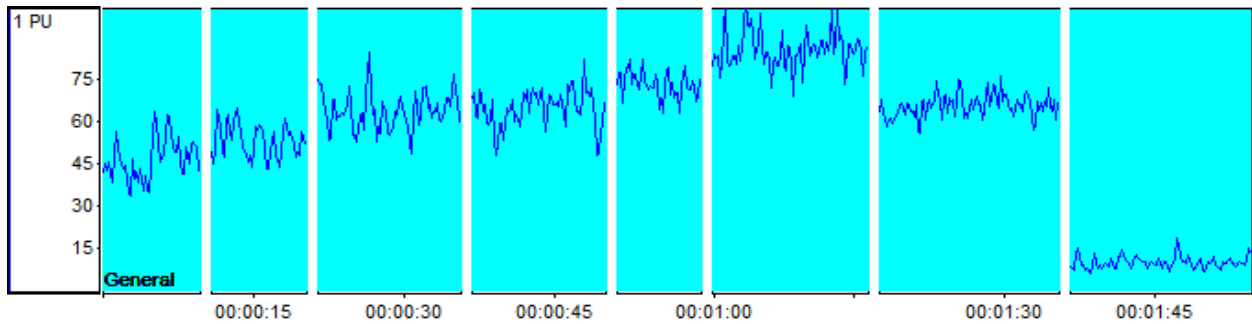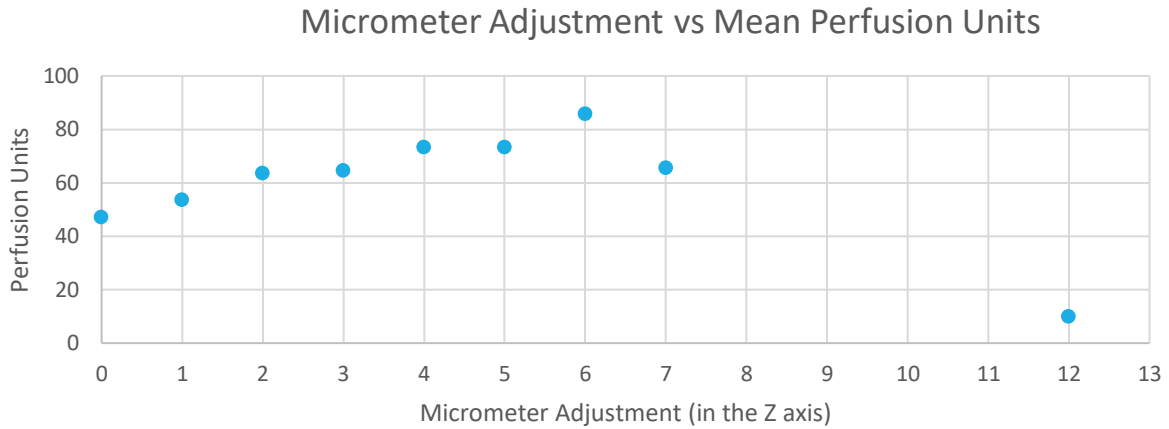
Figure 3: Graph and Perisoft Software output of Doppler Positioning Experiment.

Doppler Flowmetry Readings

The Perimed 5001 is a Laser Doppler unit that specializes in taking precise blood perfusion readings through the placement of the Doppler probe. This unit measures the Doppler shift that is reflected off moving red blood cells and transforms it into an electronic signal that is displayed on the Perimed Software. The Doppler Probe was held via a specialized probe holder to stabilize the probe to prevent it from exerting unwanted pressure on regions of interest. Prior to performing blood perfusion recordings of the two cohorts, sample readings were recorded on pilot animals where the probe was lowered approximately in 1mm intervals starting from being positioned right above the nerve. These pilot reading curves validated the chosen height of the

probe placement (Figure 3). The probe was held approximately 1-2 mm above sites of recording to ensure that blood perfusion readings were originating from the correct structures of interest. The probe angle was held consistent throughout all recordings to ensure the most accurate signals. Readings were taken over a 30 second period. The Perisoft software was used to record data in perfusion units and perform an initial analysis of the various readings. After the sciatic nerve is exposed, Doppler Flowmetry readings were recorded by placing the probe on the surrounding muscle before and after decompression. The probe recorded blood perfusion for the proximal and distal portions of the sciatic nerve before and after decompression of the nerve. Measurements were also taken at the one-week time point and six-week time point for muscle, proximal, and distal regions. At the endpoint of the one-week and six-week cohorts, blood perfusion readings of the muscle, proximal, and distal regions were taken from the contralateral side to function as controls.

Immunohistochemistry Staining

During the terminal surgeries of all fourteen rats, the sciatic nerve, along with some of its nerve bed, was extracted and stored in 4% paraformaldehyde and was allowed to sit in this solution for 24-48hrs to allow for proper fixation. After 24-48 hours, the nerves were placed in 70% ethanol for preservation. The nerve tissue was then sectioned into three regions: distal cross-section, proximal cross-section, and a longitudinal section. Standard paraffin embedding protocols were followed to allow for proper sectioning on a microtome where sectioned tissue was placed on slides.

Sections were deparaffinized through three washes in various propar solutions, two washes in 100% EtOH solution, one wash in 95% EtOH solution, and finally stored in distilled

water. Antigen retrieval was performed by placing slides in a 6.0 pH citrate buffer and allowed steam up to 20 minutes at 95-100 degrees Celsius in a vegetable steamer. After slides were removed from the vegetable steamer, they were allowed to cool off through running tap water on the slides before moving onto immunohistochemical stanning protocols. This following protocol was adapted from "Immunofluorescence Staining of Paraffin Sections Step by Step" by (Zaqout et al., 2020).

Slides were stood up against a surface to allow the sections to dry before application of a hydrophobic barrier pen around the section. Once the barrier pen was used, the slides were rinsed with PBS, twice for two minutes. Then the slides were washed with PBS for 10 minutes. Finally, slides were then washed with a mixture of PBS/gelatin/Triton .25% solution twice for 10 minutes.

The slides were then placed in a humid box where a small amount of water soaked foam sponges at the bottom of the humid box. 190 microliters of 5% BSA solution was added to slides as a blocking step and the humid box was the closed for 60 minutes and kept at room temperature.

The slides are then taken out of the humid box where the BSA solution was removed via paper towels. 190 microliters of the primary antibody solutions were placed on each slide. Slides were returned to the humid box and closed where the box was left overnight at room temperature.

In the following day, slides were removed from the humid box and washed with PBS twice for 10 minutes and PBS/gelatin/Triton .25% for 10 minutes. Again, excess liquid was

removed via paper towels. Following this washing step, slides were returned to the humid box where secondary antibody solution was placed and allowed to spread out on all slides.

The final rinsing steps are as follows: PBS, three times for ten minutes, a 10mM CuSO4/50 mM NH4Cl solution for ten minutes, and then finally a rinse of distilled water. Slides were then allowed to dry for a short period of time and Shandon ImmunoMount was placed on each slide with a coverslip over the section to seal the section. These slides were allowed to dry in the dark for 24 hours before any imaging occurred. Images were acquired via confocal microscope at the Altman Clinical and Translational Research Institute.

Data Analysis

Subsections of the 30 second recording interval where perfusion readings were consistent were used for data analysis. The Perimed Software analyzed mean perfusion levels over the selected intervals. Outliers were then removed if they exceeded the lower bound of 1.5 - (Interquartile Range*1.5) or the upper bound of Q3 + (Interquartile Range*1.5). In total, 10 data points were removed as they were calculated to be an outlier via our exclusion criterion. All consequent data analysis was performed through IBM SPSS Statistics Software. Two-Way ANOVA and Tukey Honest Significant Difference Tests were used to analyze potential significant differences. Our threshold was set at p <.05 for all statistical tests. Initially, pre-decompression perfusion was compared with T0 (immediately following decompression) perfusion. Then, pre-decompression and T0 perfusion readings were compared with T2 (six-weeks after decompression) and T1 (one-week after decompression) perfusion readings. Contralateral control values were also compared to pre-decompression values.

In our data analysis, comparisons between regional groups: muscle vs proximal, muscle vs distal, distal vs proximal, were not examined. Only different configurations/decompression states in regional groups were analyzed against other configuration/decompression states in the same regional group.
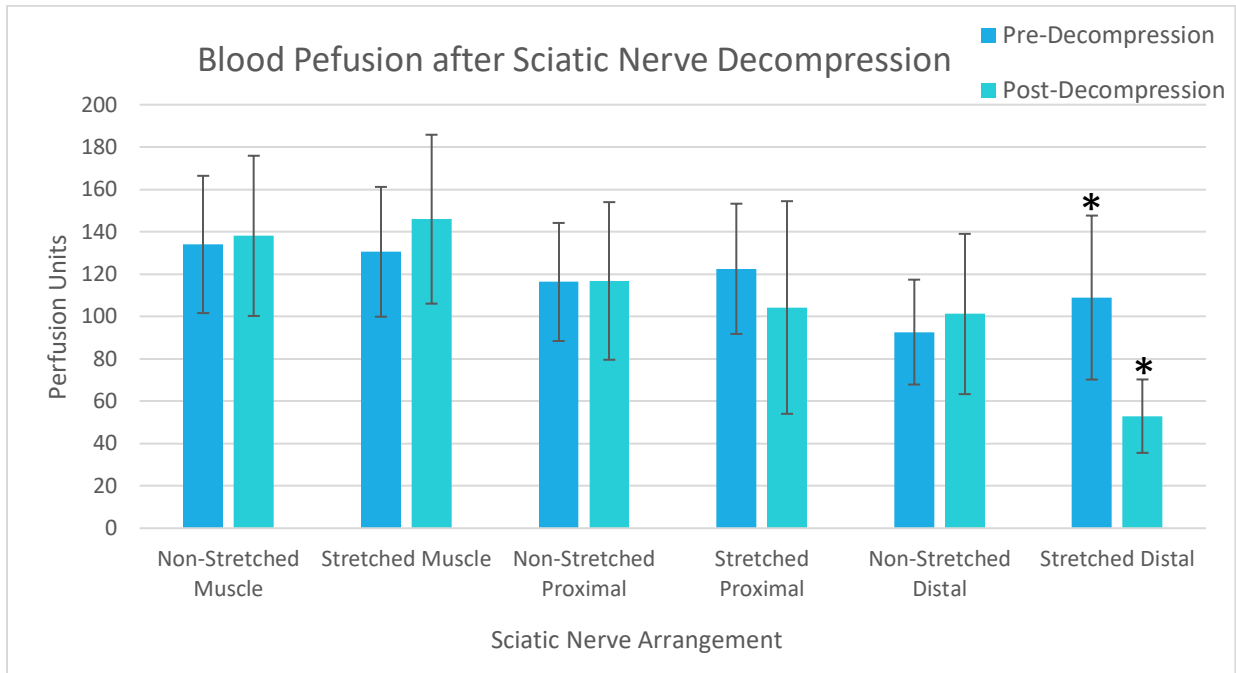
Figure 4: Mean blood perfusion levels $\pm$ standard deviations before and after peripheral nerve decompression. N=14. Asterisks signify statistical differences.
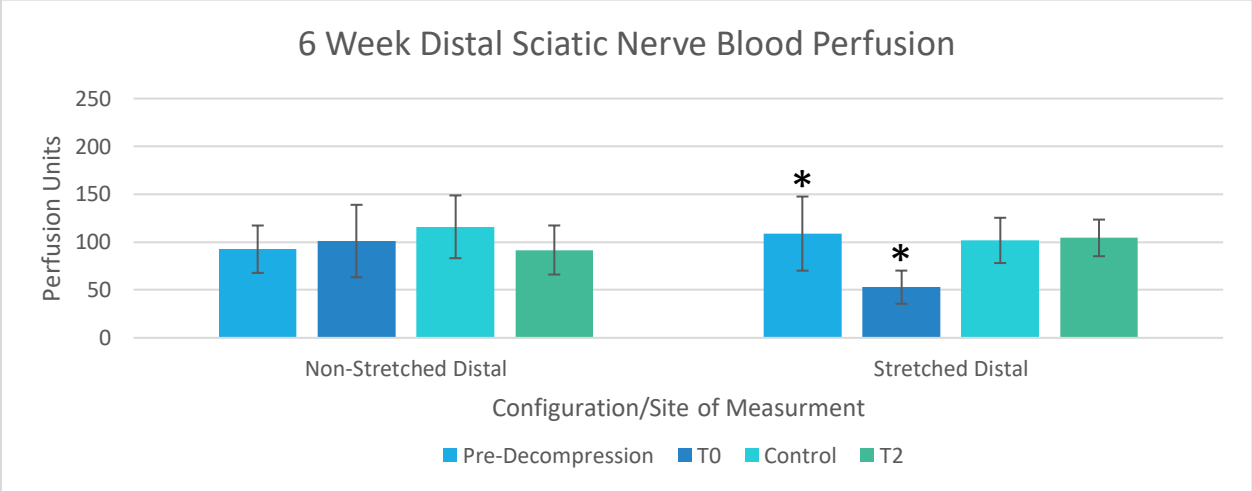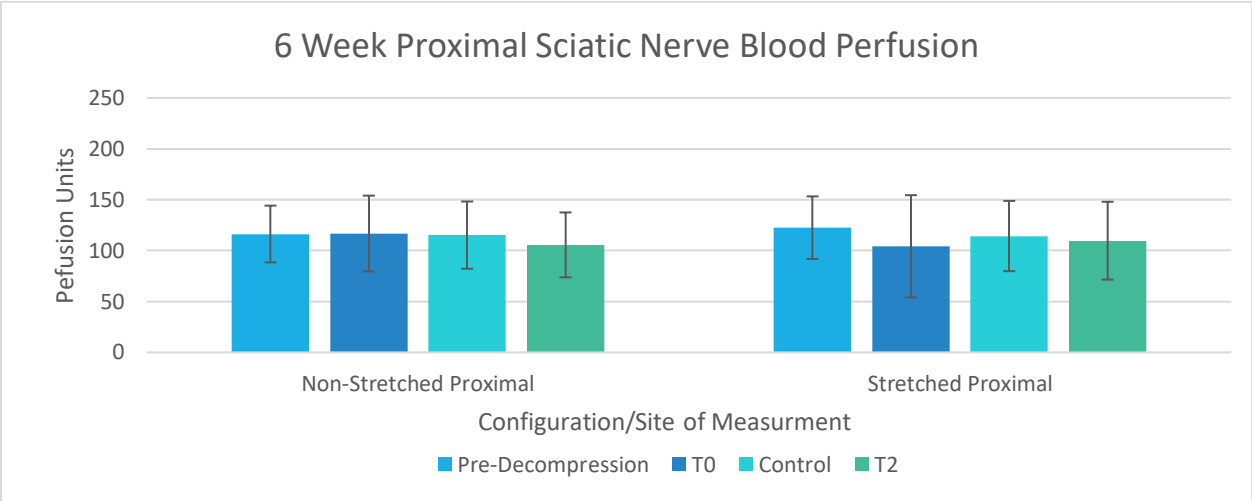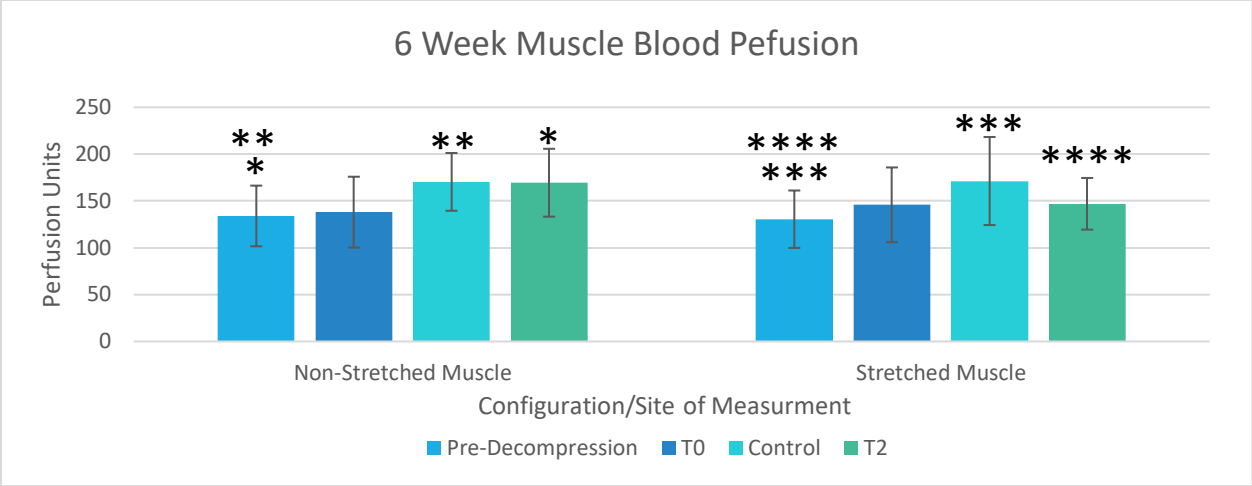
Figure 5: Initial mean perfusion data ± standard deviations compared with six-week timepoint readings. Pre-Decompression and T0: N=14, Control and T2: N=10. T0 readings were recorded right after decompression, control and T2 readings were recorded 6 weeks after decompression. Asterisks signify significant differences.
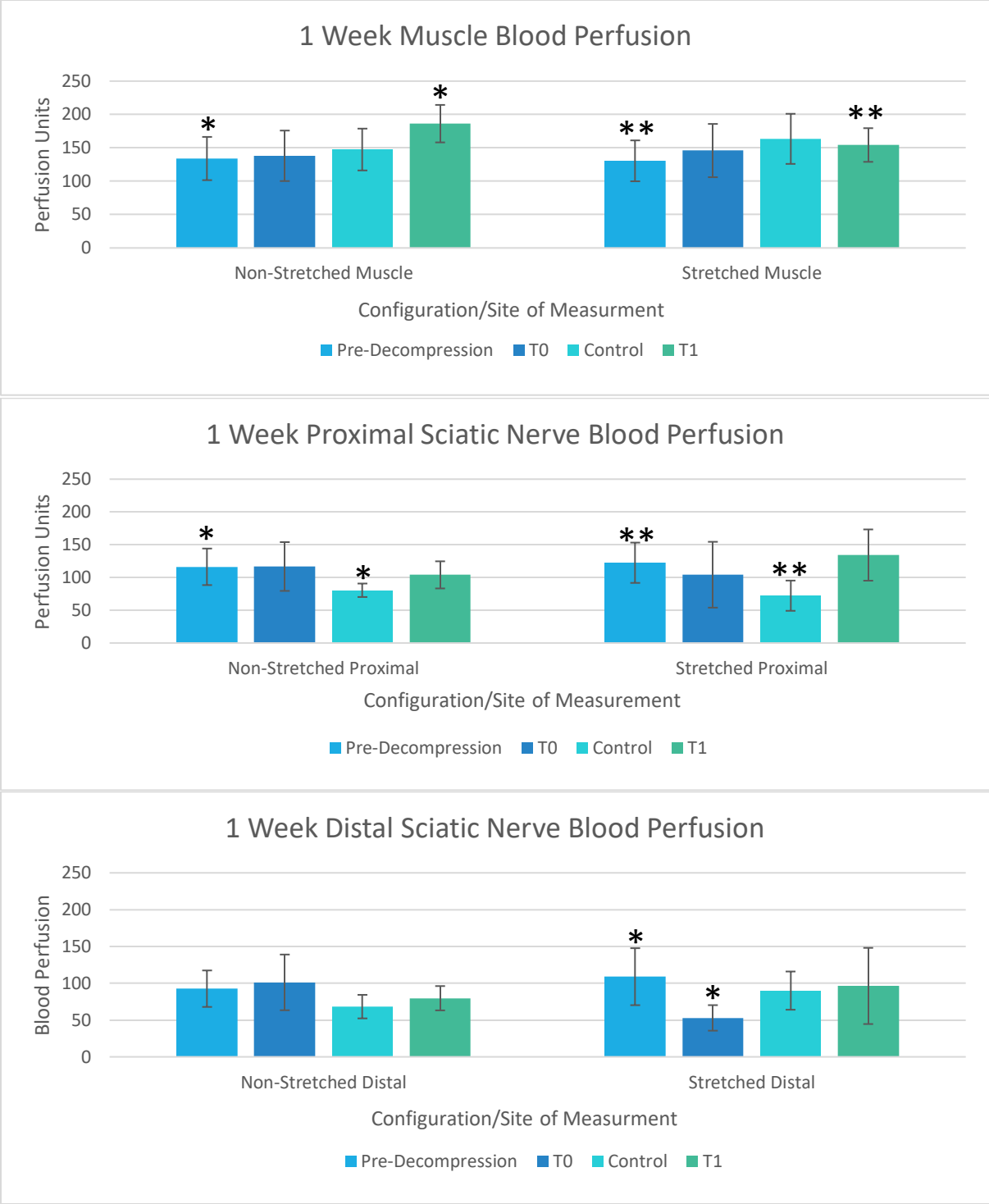
Figure 6: Initial mean perfusion data ± standard deviations compared to one-week time point readings. Pre-Decompression and T0: N=14, Control and T1: N=4. T0 readings were recorded right after decompression, control and T1 readings were recorded 1 week after decompression. Asterisks signify significant differences.

Muscle

Two-Way ANOVA analysis revealed no effect of time, stretch, or time and stretch between pre-decompression blood perfusion levels and post-decompression (T0) (Figure 4, Table S1). Two-Way ANOVA analysis of initial decompression data compared to one-week data revealed an effect of time (p= .031) (Figure 6, Table S2). Tukey tests revealed significant differences when comparing pre-decompression levels versus one-week (T1) post-decompression levels (p=.023) and six week (T2) post-decompression levels (p= .035) (Figure 5, Figure 6, Table S3).

Two-Way ANOVA analysis of pre-decompression versus six-week controls revealed an effect of time (p= <.001) (Figure 5, Table S5). This phenomenon was not observed when comparing pre-decompression and one-week controls (Figure 6, Table S5).

Due to the nature of the experimental time-points, animals could have grown a significant amount explaining the increase in blood perfusion observed at T1 (one-week) post-decompression, T2 (six-week) post-decompression, and the 6-week control time-point. As predicted, muscle blood perfusion was not impacted negatively due to nerve manipulations. While we controlled surgical effects, there might have been an effect of anesthesia on blood perfusion during surgery.

Proximal

Two-Way ANOVA and Tukey HSD analysis of the proximal sciatic nerve revealed no significant differences between pre-decompression blood perfusion versus T0 post-decompression, T1 post-decompression, and T2 post decompression blood perfusion levels (Figure 4, Figure 5, Figure 6, Table S1, Table S2, Table S4).

Two-Way ANOVA analysis of pre-decompression perfusion versus six-week contralateral control perfusion revealed no significant interaction of time, stretch, and both time and stretch (Table S5). However, an effect of time was observed between pre-decompression perfusion versus one-week contralateral control perfusion (p= <.01) (Table S5).

Perfusion of the proximal sciatic nerve on the experimental side was not affected after decompression. Unexpectedly, we observed lower blood perfusion levels on one-week contralateral controls compared to pre-decompression levels. The sample size for the one-week cohort was small (N=4), so this dataset has low power. Larger cohorts may reveal contralateral control levels to be similar or higher to pre-decompression levels.

Distal

Two-Way ANOVA Analysis revealed an effect of time but not stretch when comparing pre-decompression versus T0 post-decompression (p=.1) (Figure 4, Table S1). An interaction ANOVA effect of time-point and stretch was observed (p=<.001) (Figure 4, Table S1). Tukey analysis revealed differences between Stretched T0 and all other groups besides Stretched T1 (Figure 5, Figure 6). All relevant significance values are reported in Table S4.

The distal portion of the sciatic nerve is affected the most after peripheral nerve decompression. Regional differences in proximal and distal ends of the sciatic nerve have been identified, where there is a convergence of vessels in the distal portion (T. M. Saffari, Mathot, Bishop, et al., 2020). Stretch imposed on sciatic nerve was linked to higher levels of strain in distal regions as well (I. M. Foran et al., 2018). Finally, the procedure of peripheral nerve decompression has the potential to separate the nerve from its external blood supply. The combination of strain, converging vascularity, and separation from the external blood supply could explain the drop in blood perfusion observed in the stretched distal sciatic nerve post-

decompression. We observed blood perfusion recovery of the stretched distal sciatic nerve at both one-week and six-week timepoints. We could attribute this to a certain level of vascular remodeling that restores vascular function to normal levels.

Immunohistochemistry Staining

After all surgeries were completed, about 55 samples were all fixed in 4% paraformaldehyde and then stored in 70% ethanol for storage. Tissues were processed and then embedded in paraffin prior to sectioning and staining. Imaging and analysis of stained images represents future work.

Limitations

We observed recovery of blood perfusion at the distal sciatic nerve at the six-week timepoint. We used a small cohort of four rats to see if that recovery was present at one week. Although we observed vascular recovery, a large cohort to analyze recovery of blood perfusion would have provided us more power in our statistical analysis.

Through our experiments, we observe that peripheral nerve decompression causes a significant decrease in the distal sciatic nerve when it under tension. However, this decompression procedure was performed on healthy nerves. In other words, this study's focus was to isolate the effects of decompression. This study does not analyze the effects of peripheral nerve decompression on injured nerves.

CONCLUSION

In this experiment, we discovered how peripheral nerve decompression effects the vascular function of peripheral nerves such as the sciatic nerve. We present evidence that this procedure causes a significant decrease in blood perfusion levels in the distal sciatic nerve when it is stretched. These results are in parallel with other findings that observe mechanical strain in the distal portion of peripheral nerves in general. Although vascular function returns to normal after six weeks, these discoveries are crucial to further our understanding on how certain surgical procedures can cause unintended effects on biomechanics and vascularity. As discussed above, a key limitation of this study is that nerve decompression was performed on healthy nerves, not injured nerves. This study isolates only the effects of decompression and does not analyze how vascular function changes with injured nerves or how vascular function changes when peripheral nerve decompression is performed on injured nerves.

Future aims for this project would be to analyze blood perfusion in nerves that are in injured states. For example, ligations could be placed around the sciatic nerve simulating peripheral nerve compression. Vascularity could then be recorded at various time points such as: pre-compression, post-compression, and post-decompression. This would allow for a holistic understanding on how blood perfusion varies between injury and therapy.

Vascular remodeling, or how the vascular system changes, after nerve manipulations can be validated through Immunohistochemistry. The experimental aim should be to effectively stain for vascular remodeling which be accomplished using different antibodies. Confirming the presence of vascular remodeling would provide key insights on the plasticity of the vascular system in general.

This thesis is currently being prepared for submission for publication of the material. Patel, Nevil; Wu, Yuanshan; Shah, Sameer. "Analysis of Vascular Changes After Peripheral Nerve Decompression." The thesis author was the primary investigator and author of this material.

REFERENCES

Adams, R. H., & Eichmann, A. (2010). Axon Guidance Molecules in Vascular Patterning. *Cold Spring Harbor Perspectives in Biology*, *2*(5), a001875–a001875. https://doi.org/10.1101/cshperspect.a001875

Aleem, A. W., Krogue, J. D., & Calfee, R. P. (2014). Outcomes of Revision Surgery for Cubital Tunnel Syndrome. *The Journal of Hand Surgery*, *39*(11), 2141–2149. https://doi.org/10.1016/j.jhsa.2014.07.013

Alvites, R., Rita Caseiro, A., Santos Pedrosa, S., Vieira Branquinho, M., Ronchi, G., Geuna, S., Varejão, A. S. P., & Colette Maurício, A. (2018). Peripheral nerve injury and axonotmesis: State of the art and recent advances. *Cogent Medicine*, *5*(1), 1466404. https://doi.org/10.1080/2331205X.2018.1466404

Arányi, Z., Csillik, A., Dévay, K., & Rosero, M. (2018). Ultrasonographic demonstration of intraneural neovascularization after penetrating nerve injury. *Muscle & Nerve*, *57*(6), 994–999. https://doi.org/10.1002/mus.26065

Best, T., & Mackinnon, S. (1994). Peripheral Nerve Revascularization: A Current Literature Review. *Journal of Reconstructive Microsurgery*, *10*(03), 193–204. https://doi.org/10.1055/s-2007-1006587

Burahee, A. S., Sanders, A. D., Shirley, C., & Power, D. M. (2021). Cubital tunnel syndrome. *EFORT Open Reviews*, *6*(9), 743–750. https://doi.org/10.1302/2058-5241.6.200129

Burnett, M. G., & Zager, E. L. (2004). Pathophysiology of peripheral nerve injury: a brief review. *Neurosurgical Focus*, *16*(5), 1–7. https://doi.org/10.3171/foc.2004.16.5.2

Caillaud, M., Richard, L., Vallat, J.-M., Desmoulière, A., & Billet, F. (2019). Peripheral nerve regeneration and intraneural revascularization. *Neural Regeneration Research*, *14*(1), 24. https://doi.org/10.4103/1673-5374.243699

Carroll, A. S., & Simon, N. G. (2020). Current and future applications of ultrasound imaging in peripheral nerve disorders. *World Journal of Radiology*, *12*(6), 101–129. https://doi.org/10.4329/wjr.v12.i6.101

Castets, M., & Mehlen, P. (2010). Netrin-1 role in angiogenesis: To be or not to be a pro-angiogenic factor? *Cell Cycle*, *9*(8), 1466–1471. https://doi.org/10.4161/cc.9.8.11197

Čebašek, V., & Ribarič, S. (2016). Changes in the Capillarity of the Rat Extensor Digitorum Longus Muscle 4 Weeks after Nerve Injury Studied by 2D Measurement Methods. *Cells Tissues Organs*, *201*(3), 211–219. https://doi.org/10.1159/000444140

Chhabra, A., Ahlawat, S., Belzberg, A., & Andreseik, G. (2014). Peripheral nerve injury grading simplified on MR neurography: As referenced to Seddon and Sunderland classifications.

Indian Journal of Radiology and Imaging, *24*(03), 217–224. https://doi.org/10.4103/0971-3026.137025

Costigan, M., Mannion, R. J., Kendall, G., Lewis, S. E., Campagna, J. A., Coggeshall, R. E., Meridith-Middleton, J., Tate, S., & Woolf, C. J. (1998). Heat Shock Protein 27: Developmental Regulation and Expression after Peripheral Nerve Injury. *The Journal of Neuroscience*, *18*(15), 5891–5900. https://doi.org/10.1523/JNEUROSCI.18-15-05891.1998

Ding, X., Tang, J., Hua, Y., Su, J., Zhang, P., Zhu, X., Wu, L., Niu, Q., & Xiao, H. (2009). Expression of VEGF and neural repair after alprostadil treatment in a rat model of sciatic nerve crush injury. *Neurology India*, *57*(4), 387. https://doi.org/10.4103/0028-3886.55583

Fagrell, B., & Nilsson, G. (1995). Advantages and Limitations of One-Point Laser Doppler Perfusion Monitoring in Clinical Practice. *Vascular Medicine Review*, *vmr-6*(2), 97–101. https://doi.org/10.1177/1358863X9500600202

Fang, Z., Ge, X., Chen, X., Xu, Y., Yuan, W.-E., & Ouyang, Y. (2020). Enhancement of sciatic nerve regeneration with dual delivery of vascular endothelial growth factor and nerve growth factor genes. *Journal of Nanobiotechnology*, *18*(1), 46. https://doi.org/10.1186/s12951-020-00606-5

Foran, I. M., Hussey, V., Patel, R. A., Sung, J., & Shah, S. B. (2018). Native paraneurial tissue and paraneurial adhesions alter nerve strain distribution in rat sciatic nerves. *Journal of Hand Surgery (European Volume)*, *43*(3), 316–323. https://doi.org/10.1177/1753193417734433

Foran, I., Vaz, K., Sikora-Klak, J., Ward, S. R., Hentzen, E. R., & Shah, S. B. (2016). Regional Ulnar Nerve Strain Following Decompression and Anterior Subcutaneous Transposition in Patients With Cubital Tunnel Syndrome. *The Journal of Hand Surgery*, *41*(10), e343–e350. https://doi.org/10.1016/j.jhsa.2016.07.095

Freund, G., Dafotakis, M., Bahm, J., & Beier, J. P. (2021). Treatment of Peripheral Nerve Compression Syndromes of the Upper Extremities: a Systematic Review. *Zeitschrift Für Orthopädie Und Unfallchirurgie*. https://doi.org/10.1055/a-1498-3197

Gao, Y., Weng, C., & Wang, X. (2013). Changes in nerve microcirculation following peripheral nerve compression. *Neural Regeneration Research*, *8*(11), 1041–1047. https://doi.org/10.3969/j.issn.1673-5374.2013.11.010

Geraldo, S., & Gordon-Weeks, P. R. (2009). Cytoskeletal dynamics in growth-cone steering. *Journal of Cell Science*, *122*(20), 3595–3604. https://doi.org/10.1242/jcs.042309

Gordon, T. (2020). Peripheral Nerve Regeneration and Muscle Reinnervation. *International Journal of Molecular Sciences*, *21*(22), 8652. https://doi.org/10.3390/ijms21228652

Guru, A., Kumar, N., Ravindra Shanthakumar, S., Patil, J., Nayak Badagabettu, S., Aithal Padur, A., & Nelluri, V. M. (2015). Anatomical Study of the Ulnar Nerve Variations at High Humeral Level and Their Possible Clinical and Diagnostic Implications. *Anatomy Research International*, *2015*, 1–4. https://doi.org/10.1155/2015/378063

HOBSON, M. I., GREEN, C. J., & TERENGHI, G. (2000). VEGF enhances intraneural angiogenesis and improves nerve regeneration after axotomy. *Journal of Anatomy*, *197*(4), 591–605. https://doi.org/10.1046/j.1469-7580.2000.19740591.x

Huang, C.-W., Hsueh, Y.-Y., Huang, W.-C., Patel, S., & Li, S. (2019). Multipotent vascular stem cells contribute to neurovascular regeneration of peripheral nerve. *Stem Cell Research & Therapy*, *10*(1), 234. https://doi.org/10.1186/s13287-019-1317-7

Jou, I.-M., Lai, K.-A., Shen, C.-L., & Yamano, Y. (2000). Changes in conduction, blood flow, histology, and neurological status following acute nerve-stretch injury induced by femoral lengthening. *Journal of Orthopaedic Research*, *18*(1), 149–155. https://doi.org/10.1002/jor.1100180121

Large, J., & Tyler, K. R. (1985). Changes in capillary distribution in rat fast muscles following nerve crush and reinnervation. *The Journal of Physiology*, *362*(1), 13–21. https://doi.org/10.1113/jphysiol.1985.sp015659

Li, M., He, Q., Hu, Z., Chen, S., Lv, Y., Liu, Z., Wen, Y., & Peng, T. (2015). Applied anatomical study of the vascularized ulnar nerve and its blood supply for cubital tunnel syndrome at the elbow region. *Neural Regeneration Research*, *10*(1), 141. https://doi.org/10.4103/1673-5374.150723

Liu, S., Liu, Y., Zhou, L., Li, C., Zhang, M., Zhang, F., Ding, Z., Wen, Y., & Zhang, P. (2021). XT-type DNA hydrogels loaded with VEGF and NGF promote peripheral nerve regeneration *via* a biphasic release profile. *Biomaterials Science*, *9*(24), 8221–8234. https://doi.org/10.1039/D1BM01377G

Long, Q., Wu, B., Yang, Y., Wang, S., Shen, Y., Bao, Q., & Xu, F. (2021). Nerve guidance conduit promoted peripheral nerve regeneration in rats. *Artificial Organs*, *45*(6), 616–624. https://doi.org/10.1111/aor.13881

Maugeri, G., D'Agata, V., Trovato, B., Roggio, F., Castorina, A., Vecchio, M., di Rosa, M., & Musumeci, G. (2021). The role of exercise on peripheral nerve regeneration: from animal model to clinical application. *Heliyon*, *7*(11), e08281. https://doi.org/10.1016/j.heliyon.2021.e08281

Menorca, R. M. G., Fussell, T. S., & Elfar, J. C. (2013). Nerve Physiology. *Hand Clinics*, *29*(3), 317–330. https://doi.org/10.1016/j.hcl.2013.04.002

Modrak, M., Talukder, M. A. H., Gurgenashvili, K., Noble, M., & Elfar, J. C. (2020). Peripheral nerve injury and myelination: Potential therapeutic strategies. *Journal of Neuroscience Research*, *98*(5), 780–795. https://doi.org/10.1002/jnr.24538

Mohammadi, R., Ahsan, S., Masoumi, M., & Amini, K. (2013). Vascular endothelial growth factor promotes peripheral nerve regeneration after sciatic nerve transection in rat. *Chinese Journal of Traumatology = Zhonghua Chuang Shang Za Zhi*, *16*(6), 323–329.

Moncion, A., Lin, M., O'Neill, E. G., Franceschi, R. T., Kripfgans, O. D., Putnam, A. J., & Fabiilli, M. L. (2017). Controlled release of basic fibroblast growth factor for angiogenesis using acoustically-responsive scaffolds. *Biomaterials*, *140*, 26–36. https://doi.org/10.1016/j.biomaterials.2017.06.012

Muangsanit, P., Shipley, R. J., & Phillips, J. B. (2018). Vascularization Strategies for Peripheral Nerve Tissue Engineering. *The Anatomical Record*, *301*(10), 1657–1667. https://doi.org/10.1002/ar.23919

Nam, A. S., Easow, J. M., Chico-Calero, I., Villiger, M., Welt, J., Borschel, G. H., Winograd, J. M., Randolph, M. A., Redmond, R. W., & Vakoc, B. J. (2018). Wide-Field Functional Microscopy of Peripheral Nerve Injury and Regeneration. *Scientific Reports*, *8*(1), 14004. https://doi.org/10.1038/s41598-018-32346-w

Niu, G., & Chen, X. (2010). Vascular Endothelial Growth Factor as an Anti-Angiogenic Target for Cancer Therapy. *Current Drug Targets*, *11*(8), 1000–1017. https://doi.org/10.2174/138945010791591395

Orfahli, L., Rezaei, M., Crawford, A. V., Annunziata, M. J., Ordenana, C., Figueroa, B., Silver, J., Rampazzo, A., & Gharb, B. B. (2020). Histomorphometry in Peripheral Nerve Regeneration: Experimental Comparison of Different Axon Counting Methods. *Plastic and Reconstructive Surgery - Global Open*, *8*(9S), 106–107. https://doi.org/10.1097/01.GOX.0000720864.51322.ad

Padua, L., Liotta, G., di Pasquale, A., Granata, G., Pazzaglia, C., Caliandro, P., & Martinoli, C. (2012). Contribution of ultrasound in the assessment of nerve diseases. *European Journal of Neurology*, *19*(1), 47–54. https://doi.org/10.1111/j.1468-1331.2011.03421.x

Podhajsky, R. J., & Myers, R. R. (1993). The vascular response to nerve crush: relationship to Wallerian degeneration and regeneration. *Brain Research*, *623*(1), 117–123. https://doi.org/10.1016/0006-8993(93)90018-I

Prevel, C. D., Matloub, H. S., Ye, Z., Sanger, J. R., & John Yousif, N. (1993). The extrinsic blood supply of the ulnar nerve at the elbow: An anatomic study. *The Journal of Hand Surgery*, *18*(3), 433–438. https://doi.org/10.1016/0363-5023(93)90086-I

Rajan, V., Varghese, B., van Leeuwen, T. G., & Steenbergen, W. (2009). Review of methodological developments in laser Doppler flowmetry. *Lasers in Medical Science*, *24*(2), 269–283. https://doi.org/10.1007/s10103-007-0524-0

Rechthand, E., & Rapoport, S. I. (1987). Regulation of the microenvironment of peripheral nerve: Role of the blood-nerve barrier. *Progress in Neurobiology*, *28*(4), 303–343. https://doi.org/10.1016/0301-0082(87)90006-2

Renno, W. M., Benov, L., & Khan, K. M. (2017). Possible role of antioxidative capacity of (−)-epigallocatechin-3-gallate treatment in morphological and neurobehavioral recovery after sciatic nerve crush injury. *Journal of Neurosurgery: Spine*, *27*(5), 593–613. https://doi.org/10.3171/2016.10.SPINE16218

Rotshenker, S. (2011). Wallerian degeneration: the innate-immune response to traumatic nerve injury. *Journal of Neuroinflammation*, *8*(1), 109. https://doi.org/10.1186/1742-2094-8-109

Rundquist, I., Smith, Q. R., Michel, M. E., Ask, P., Oberg, P. A., & Rapoport, S. I. (1985). Sciatic nerve blood flow measured by laser Doppler flowmetry and [14C]iodoantipyrine. *American Journal of Physiology-Heart and Circulatory Physiology*, *248*(3), H311–H317. https://doi.org/10.1152/ajpheart.1985.248.3.H311

Saffari, T., Bedar, M., Hundepool, C., Bishop, A., & Shin, A. (2020). The role of vascularization in nerve regeneration of nerve graft. *Neural Regeneration Research*, *15*(9), 1573. https://doi.org/10.4103/1673-5374.276327

Saffari, T. M., Mathot, F., Bishop, A. T., & Shin, A. Y. (2020). New methods for objective angiogenesis evaluation of rat nerves using microcomputed tomography scanning and conventional photography. *Microsurgery*, *40*(3), 370–376. https://doi.org/10.1002/micr.30537

Saffari, T. M., Mathot, F., Friedrich, P. F., Bishop, A. T., & Shin, A. Y. (2020). Revascularization patterns of nerve allografts in a rat sciatic nerve defect model. *Journal of Plastic, Reconstructive & Aesthetic Surgery*, *73*(3), 460–468. https://doi.org/10.1016/j.bjps.2019.11.048

Said, G. (2007). Diabetic neuropathy—a review. *Nature Clinical Practice Neurology*, *3*(6), 331–340. https://doi.org/10.1038/ncpneuro0504

Schmidt, C. E., & Leach, J. B. (2003). Neural Tissue Engineering: Strategies for Repair and Regeneration. *Annual Review of Biomedical Engineering*, *5*(1), 293–347. https://doi.org/10.1146/annurev.bioeng.5.011303.120731

SEDDON, H. J. (1943). THREE TYPES OF NERVE INJURY. *Brain*, *66*(4), 237–288. https://doi.org/10.1093/brain/66.4.237

Sun, X., Zhu, Y., Yin, H., Guo, Z., Xu, F., Xiao, B., Jiang, W., Guo, W., Meng, H., Lu, S., Wang, Y., & Peng, J. (2018). Differentiation of adipose-derived stem cells into Schwann cell-like cells through intermittent induction: potential advantage of cellular transient memory function. *Stem Cell Research & Therapy*, *9*(1), 133. https://doi.org/10.1186/s13287-018-0884-3

SUNDERLAND, S. (1951). A CLASSIFICATION OF PERIPHERAL NERVE INJURIES PRODUCING LOSS OF FUNCTION. *Brain*, *74*(4), 491–516. https://doi.org/10.1093/brain/74.4.491

Vela, F., Martínez-Chacón, G., Ballestín, A., Campos, J., Sánchez-Margallo, F., & Abellán, E. (2020). Animal models used to study direct peripheral nerve repair: a systematic review. *Neural Regeneration Research*, *15*(3), 491. https://doi.org/10.4103/1673-5374.266068

Wang, M. L., Rivlin, M., Graham, J. G., & Beredjiklian, P. K. (2019). Peripheral nerve injury, scarring, and recovery. *Connective Tissue Research*, *60*(1), 3–9. https://doi.org/10.1080/03008207.2018.1489381

Wu, P., Tong, Z., Luo, L., Zhao, Y., Chen, F., Li, Y., Huselstein, C., Ye, Q., Ye, Q., & Chen, Y. (2021). Comprehensive strategy of conduit guidance combined with VEGF producing Schwann cells accelerates peripheral nerve repair. *Bioactive Materials*, *6*(10), 3515–3527. https://doi.org/10.1016/j.bioactmat.2021.03.020

Xia, B., & Lv, Y. (2018). Dual-delivery of VEGF and NGF by emulsion electrospun nanofibrous scaffold for peripheral nerve regeneration. *Materials Science and Engineering: C*, *82*, 253–264. https://doi.org/10.1016/j.msec.2017.08.030

Zamir, M., Twynstra, J., Vercnocke, A. J., Welch, I., Jorgensen, S. M., Ritman, E. L., Holdsworth, D. W., & Shoemaker, J. K. (2012). Intrinsic microvasculature of the sciatic nerve in the rat. *Journal of the Peripheral Nervous System*, *17*(4), 377–384. https://doi.org/10.1111/j.1529-8027.2012.00435.x

Zaqout, S., Becker, L.-L., & Kaindl, A. M. (2020). Immunofluorescence Staining of Paraffin Sections Step by Step. *Frontiers in Neuroanatomy*, *14*. https://doi.org/10.3389/fnana.2020.582218

Zhang, J. C., Zheng, G. F., Wu, L., Ou Yang, L. Y., & Li, W. X. (2014). Bone marrow mesenchymal stem cells overexpressing human basic fibroblast growth factor increase vasculogenesis in ischemic rats. *Brazilian Journal of Medical and Biological Research*, *47*(10), 886–894. https://doi.org/10.1590/1414-431X20143765

Table S1: Two-Way ANOVA analysis of Pre-Decompression vs T0 post-decompression blood perfusion. P-values are reported, and significant values are highlighted.

Muscle Pre-Decompression vs T0 ANOVA	Significance
Time	0.314
Stretch	0.819
Time*Stretch	0.557
Proximal Pre-Decompression vs T0 ANOVA	Significance
Time	0.68
Stretch	0.941
Time*Stretch	0.511
Distal Pre-Decompression vs T0 ANOVA	Significance
Time	0.1
Stretch	0.076
Time*Stretch	<.001

Table S2: Two-Way ANOVA analysis of initial decompression data (pre-decompression and T0) versus 6-Week and 1-Week Post-Decompression data. P-values are reported, and significant values are highlighted.

Muscle 6 Week ANOVA	Significance
Time	0.051
Stretch	0.465
Time*Stretch	0.345
Muscle 1 Week ANOVA	Significance
Time	0.031
Stretch	0.374
Time*Stretch	0.361
Proximal 6 Week ANOVA	Significance
Time	0.501
Stretch	0.932
Time*Stretch	0.606
Proximal 1 Week ANOVA	Significance
Time	0.82
Stretch	0.522
Time*Stretch	0.374
Distal 6 Week ANOVA	Significance
Time	0.012
Stretch	0.372
Time*Stretch	<.001
Distal 1 Week ANOVA	Significance
Time	0.038
Stretch	0.63
Time*Stretch	0.002

Table S3: Tukey Honest Significant Difference Comparisons of time-points. Pre-Decompression versus T0 post-decompression and T2 (six-weeks post-decompression). Pre-Decompression versus T0 post-decompression and T1(one-week post-decompression). P-values are reported, and significant values are highlighted.

Muscle 6 Week Tukey HSD	Pre-Decompression	T0	T2
Pre-Decompression		0.56	0.035
T0	0.56		0.24
T2	0.035	0.24	
Muscle 1 Week Tukey HSD	PD	T0	T1
Pre-Decompression		0.559	0.023
T0	0.559		0.114
T1	0.023	0.114	
Proximal 6 Week Tukey HSD	Pre-Decompression	T0	T2
Pre-Decompression		0.649	0.522
T0	0.649		0.963
T2	0.522	0.963	
Proximal 1 Week Tukey HSD	Pre-Decompression	T0	T1
Pre-Decompression		0.661	0.991
T0	0.661		0.847
T1	0.991	0.847	
Distal 6 Week Tukey HSD	Pre-Decompression	T0	T2
Pre-Decompression		0.015	0.952
T0	0.015		0.06
T2	0.952	0.06	
Distal 1 Week Tukey HSD	Pre-Decompression	T0	T1
Pre-Decompression		0.029	0.65
T0	0.029		0.731
T1	0.65	0.731	

Table S4: Tukey Honest Significant Difference comparisons of stretched/non-stretched configurations linked to time-points. Initial decompression data (pre-decompression and T0) are compared against six-week decompression data (T2) and one-week decompression data (T1). P-values are reported, and significant values are highlighted.

Muscle 6 Week Comparison Tukey HSD	Non-Stretched Pre-Decompression	Non-Stretched T0	Non-Stretched T2	Stretched Pre-Decompression	Stretched T0	Stretched T2
Non-Stretched Pre-Decompression		1	0.148	1	0.943	0.951
Non-Stretched T0	1		0.258	0.993	0.991	0.991
Non-Stretched T2	0.148	0.258		0.096	0.576	0.721
Stretched Pre-Decompression	1	0.993	0.096		0.858	0.883
Stretched T0	0.943	0.991	0.576	0.858		1
Stretched T2	0.951	0.991	0.721	0.883	1	
Muscle 1 Week Comparison Tukey HSD	Non-Stretched Pre-Decompression	Non-Stretched T0	Non-Stretched T1	Stretched Pre-Decompression	Stretched T0	Stretched T1
Non-Stretched Pre-Decompression		1	0.1	1	0.942	0.906
Non-Stretched T0	1		0.156	0.993	0.991	0.962
Non-Stretched T1	0.1	0.156		0.07	0.327	0.781
Stretched Pre-Decompression	1	0.993	0.07		0.858	0.837
Stretched T0	0.942	0.991	0.327	0.857		0.998
Stretched T1	0.906	0.962	0.781	0.837	0.998	

Proximal 6 Week Comparison Tukey HSD	Non-Stretched Pre-Decompression	Non-Stretched T0	Non-Stretched T2	Stretched Pre-Decompression	Stretched T0	Stretched T2
Non-Stretched Pre-Decompression		1	0.981	0.998	0.956	0.998
Non-Stretched T0	1		0.978	0.999	0.952	0.997
Non-Stretched T2	0.981	0.978		0.875	1	1
Stretched Pre-Decompression	0.998	0.999	0.875		0.788	0.958
Stretched T0	0.956	0.952	1	0.788		0.999
Stretched T2	0.998	0.997	1	0.958	0.999	

Proximal 1 Week Comparison Tukey HSD	Non-Stretched Pre-Decompression	Non-Stretched T0	Non-Stretched T1	Stretched Pre-Decompression	Stretched T0	Stretched T1
Non-Stretched Pre-Decompression		1	1	0.999	1	0.987
Non-Stretched T0	1		0.992	0.999	0.961	0.968
Non-Stretched T1	1	0.992		0.958	1	0.878
Stretched Pre-Decompression	0.999	0.999	0.958		0.824	0.994
Stretched T0	1	0.961	1	0.824		0.754
Stretched T1	0.987	0.968	0.878	0.994	0.754	

Distal 6 Week Comparison Tukey HSD	Non-Stretched Pre-Decompression	Non-Stretched T0	Non-Stretched T2	Stretched Pre-Decompression	Stretched T0	Stretched T2
Non-Stretched Pre-Decompression		0.977	1	0.71	0.014	0.935
Non-Stretched T0	0.977		0.977	0.985	0.002	1
Non-Stretched T2	1	0.977		0.752	0.04	0.939
Stretched Pre-Decompression	0.71	0.985	0.752		<.001	0.999
Stretched T0	0.014	0.002	0.04	<.001		0.002
Stretched T2	0.935	1	0.939	0.999	0.002	
Distal 1 Week Comparison Tukey HSD	Non-Stretched Pre-Decompression	Non-Stretched T0	Non-Stretched T1	Stretched Pre-Decompression	Stretched T0	Stretched T1
Non-Stretched Pre-Decompression		0.984	0.988	0.778	0.033	1
Non-Stretched T0	0.984		0.898	0.99	0.006	1
Non-Stretched T1	0.988	0.898		0.703	0.78	0.987
Stretched Pre-Decompression	0.778	0.99	0.703		<.001	0.989
Stretched T0	0.033	0.006	0.78	<.001		0.294
Stretched T1	1	1	0.987	0.989	0.294	

Table S5: Two-Way ANOVA comparison between pre-decompression perfusion and contralateral control perfusion. P-values are reported, and significant values are highlighted.

Muscle: Pre-Decompression vs 6 Week Control ANOVA	Significance
Time	<.001
Stretch	0.903
Time*Stretch	0.835
Muscle: Pre-Decompression vs 1 Week Control ANOVA	Significance
Time	0.083
Stretch	0.632
Time*Stretch	0.458
Proximal: Pre-Decompression vs 6 Week Control ANOVA	Significance
Time	0.614
Stretch	0.773
Time*Stretch	0.699
Proximal: Pre-Decompression vs 1 Week Control ANOVA	Significance
Time	<.001
Stretch	0.927
Time*Stretch	0.517
Distal: Pre-Decompression Vs 6 Week Control ANOVA	Significance
Time	0.381
Stretch	0.909
Time*Stretch	0.104
Distal: Pre-Decompression vs 1 Week Control ANOVA	Significance
Time	0.091
Stretch	0.135
Time*Stretch	0.838